Photocatalytic inactivation of Escherichia coli bacteria in water using low pressure plasma deposited TiO2 cellulose fabric

Photocatalytic inactivation of *Escherichia coli* bacteria in water using low pressure plasma deposited TiO_2 cellulose fabric

Nicoletta De Vietro,[a] Antonio Tursi,[*b,c] Amerigo Beneduci,[b] Francesco Chidichimo,[d] Antonella Milella,[e] Francesco Fracassi,[e] Efthalia Chatzisymeon[c] and Giuseppe Chidichimo[b]

[a] Institute of Nanotechnology (Nanotec), National Research Council (CNR), c/o Department of Chemistry, University of Bari "Aldo Moro", Via Orabona 4, 70126 Bari, Italy

[b] Department of Chemistry and Chemical Technologies, University of Calabria, Via P. Bucci, Cubo 15D, 87036 Arcavacata di Rende (Cs), Italy

[c] School of Engineering, Institute for Infrastructure and Environment, University of Edinburgh, The King's Buildings, Edinburgh EH9 3JL, United Kingdom

[d] Department of Environmental and Chemical Engineering, University of Calabria, Via P. Bucci, Cubo 41B, 87036 Arcavacata di Rende (CS), Italy

[e] Department of Chemistry, University of Bari "Aldo Moro", Via Orabona 4, 70126 Bari, Italy

ABSTRACT

Fabrics obtained from cellulose spinning, extracted from Spanish broom, were coated with TiO_2 film, through the low pressure plasma sputtering technique, in order to get antibacterial activity. The obtained fabrics were used for the photocatalytic degradation of *Escherichia coli*, by irradiation with UV-light emitting diodes (UV-LED), in a batch photocatalytic reactor. Before and after functionalization treatments, cellulosic substrates were chemically characterized by X-ray photoelectron spectroscopy (XPS) analyses. Water Contact Angle (WCA) measurements allowed to obtain information about the hydrophilicity of the materials, while their antibacterial efficiency was determined at several initial concentrations (from 10^3 up to 10^8 CFU/mL) of bacteria in distilled, bottled water and synthetic wastewater. It was found that photocatalytic reactions were capable of achieving up to 100% bacterial inactivation in 1 h of treatment, following a pseudo-first order kinetic model. No bacterial regrowth was observed after photocatalytic treatments in almost all experimental conditions. In contrast, during photolytic treatment (i.e. in the absence of the TiO_2 coated fabrics) bacteria recovered their initial concentration after 3 h in the dark. Finally, the reusability of the plasma modified fibers to inactivate bacteria was studied.

Keywords: *Escherichia coli*; titania catalyst; Low pressure plasma sputtering; Titanium dioxide; water disinfection; advanced oxidation.

1. Introduction

Safe drinking water represents the greatest need for humanity. Currently, one of the major problems that must be solved, especially in underdeveloped countries, is the decontamination of water from faecal coliform bacteria.[1] Faecal coliform bacteria are a group of bacteria that comes from faecal droppings of humans, livestock and wildlife. The most common member of this category is *Escherichia coli*.

The presence of *E. coli* is used as an indicator to monitor the possible presence of other more harmful microbes, such as Giardia, Cryptosporidium and Shigella.[2]

Many methods have been used for the inactivation of microbial pollutants, such as chlorination, ozone, filtration and photocatalytic oxidation.[3] Chlorination is the most common method for the chemical disinfection of water but it also leads to the formation of carcinogenic by-products, such as trihalomethanes (THM).[4,5] Therefore, it is necessary to resort to more advanced technological methods for water disinfection, overcoming the current methods of chlorination.[3]

Conventional disinfection using UV mercury vapor lamps is an effective water remediation technology. But in the last few decades, UV light emitting diodes (UV-LEDs) have played an important role as an alternative to mercury vapor lamps, due to the absence of mercury, higher strength and flexibility, compact dimensions and large amounts of energy transmitted with less thermal energy production as waste. Furthermore, the UV-LEDs technology allows to adjust the working wavelengths and does not need heating periods. Nelson et al.[6] has demonstrated that the LEDs emitting wavelengths between 200 and 290 nm can be used for water treatment to reduce pathogens in water without formation of disinfection by-products (DBPs). In particular, experimental tests, with UV-LEDs radiation at 265 nm in ultra-pure water for 50 min exposure time, have showed a 1-2 log reduction of *E. coli* in water.[7]

Instead, Hamamoto et al.[8] applied UV-A radiation with 365 nm UVA-LEDs on *E. coli* and obtained UV dose responses of 55,263 mJ/cm^2 per log inactivation. Xiong and Hu (2013) introduced a photolytic disinfection system using 365 nm UV-LEDs, with a UV dose response as low as 229 mJ/cm^2 per log *E. coli* inactivation, showing that 365 nm UVA-LEDs alone are not effective for bacterial inactivation.[9]

For this reason, the use of photocatalysts is increasingly studied to improve the capacity of bacterial inactivation at different wavelengths and decrease the application/exposure times, but above all to use wavelengths closer to the visible region (such as UV-A), which require less UV light intensity and are potentially less damaging to the surrounding environment.

TiO_2, WO_3, CdS, SnO_2, ZnO_2, Fe_2O_3 can be used as photocatalysts but oxidation processes need high potentials in order to have the valence band location in a sufficiently positive state to allow the oxidation of organic compounds, such as TiO_2 and CdS.[10,11] In these two cases, in fact, the photogenerated holes have the ability to generate ·OH radicals with sufficient energy to trigger the oxidation reactions, but CdS does not present good stability in aqueous solutions. In this regard, several studies have focused on the photocatalytic advantages of titanium oxide against bacteria.[12]

In recent years, several studies have shown the use of superficially modified materials with TiO_2 to increase the antibacterial activity and for a greater stability of the catalyst. Janus et al.[13] studied the photocatalytic disinfection of *E. coli* by carbon modified TiO_2 in a pressure reactor with the use of five alcohols at 120 °C for 4 h, for modification purposes. Wu et al.[14] found titanium dioxide nanoparticles co-doped with nitrogen and silver as visible light driven photocatalyst for bactericidal activity against *E. coli*. Inactivation of bacteria by nanocarbon/TiO_2 composite photocatalyst[15] and titanium dioxide-coated carbon nanotubes[16,17] were also investigated in the last decades. Dagan and Tomkiewicz[18] have introduced a new method involving the use of TiO_2 aerogels for the photo-assisted oxidation of organic compounds. Sethi et al.[19] have performed vanadium modified titanium (V_2O_5/TiO_2) photocatalysts, prepared by incipient wet impregnation method, using aqueous ammonium metavanadate and anatase titania for the photocatalytic destruction of *E. coli* in water.

Based on these considerations, this work presents the first application of photocatalytic bacterial inactivation using TiO_2 coated cellulose spinning, extracted from Spanish Broom (SB).[20] This spontaneous vegetable widely spread onto the planet, offers the possibility to easily extract either the lignocellulosic or the cellulose fibers. It has been recently shown that these fibers can be used either in the pristine form to remove inorganic contaminants from water[21] or, after surface functionalization, organic pollutants from water by adsorption processes.[22, 23] Here, we have explored the possibility to use a low pressure plasma sputtering technique for the deposition of TiO_2 on Spanish Broom cellulose surface. Generally, non-equilibrium plasma processes, both at low or atmospheric pressure, are eco-friendly, versatile and, thanks to their low temperature (near to room), allow the modification of the uppermost layers of flat substrates,[24] fibers or granules,[25-29] without changing their bulk properties. Specifically, we have previously demonstrated that, feeding the discharger with metal-based precursors, anti-microbial or photocatalytic coatings can be obtained.[30, 31]

In this work, several deposition processes were optimized with the aim of obtaining the highest TiO_2 mass fraction, without deterioration of the fabric substrate and needless time consumption, using surface and morphology characterization experimental results.

Before and after the plasma treatment, in fact, all fibers were analysed by X-ray photoelectron spectroscopy (XPS), for the chemical characterization of the fiber surface. Moreover, water contact

angle (WCA) measurements have been performed to evaluate the hydrophilicity of plasma treated material.

The obtained fabrics were tested for the photocatalytic degradation of *E. coli*, by irradiation with 356 nm UV-LEDs in a batch photocatalytic reactor.

2. Materials and methods

2.1. SB fibers extraction process and fabric preparation

SB fibers were extracted by treating the raw vegetable, grown into the botanic garden of the University of Calabria, with a 5% w/w NaOH water solution for 20 minutes at 80 °C by dissolving pectin and lignin contents. After this first stage, the fiber still contains around 5% of lignin.

In order to remove these impurities, further digestion of 30 minutes is carried out at 80 °C in a diluted (0.5% w/w) NaOH water solution to prevent cellulose hydrolysis. In such a way, the content of lignin has been reduced to 1%.[20]

The fiber extracted and purified has been spinned at Linificio e Canapificio Italiano S.r.l. (Villa d'Almè (BG) – Italy), by means of standard apparatus there available, after being carded. The linear density of the yarn was about 1000 dtex (grams for 10 km). Finally, the fabric has been obtain by courtesy of Crespi 1797 S.r.l. (Ghemme (NO) – Italy), by means of their weaving apparatus.

2.2. Preparation of antimicrobial cellulosic SB fabric through plasma sputtering system

Sputtering processes were performed on a 5 cm disk of SB fabric, without any pre-treatment, in the lab scale reactor schematized in Fig. 1.

The experimental apparatus utilized for the deposition of the TiO_2 coatings (Fig. 1) consists of a cylindrical low pressure plasma reactor with an asymmetric electrode configuration (70 mm inter-electrode distance), equipped by a turbomolecular (*Pfeiffer*, TNH 521P, pumping speed 500L/h) - rotary (*Pfeiffer*, DUO 20; pumping speed, 20 m^3/h) pumping system. The pressure is measured and controlled in the 0 ÷ 133.32 Pa range with a baratron gauge (*MKS*) and an automatic throttle valve (*Pfeiffer*). The lower stainless steel circular electrode (diameter, 190 mm), on which the SB fabrics (the substrate) were positioned during the deposition process, was thermally controlled, at 25 °C, by means of a circulating water and glycol mixture, and grounded. The upper electrode, equipped with a grounded shutter, on the other hand, is a circular balanced magnetron sputtering (MS) source (*Aja Instrument*, A330; diameter, 76.2 mm), powered with 13.56 MHz radio frequency (RF) power supplies (*Advanced Energy*, CESAR 1330; power range, 0-3000 W) with automatic matching network (*Dressler*, VM 1000) units.

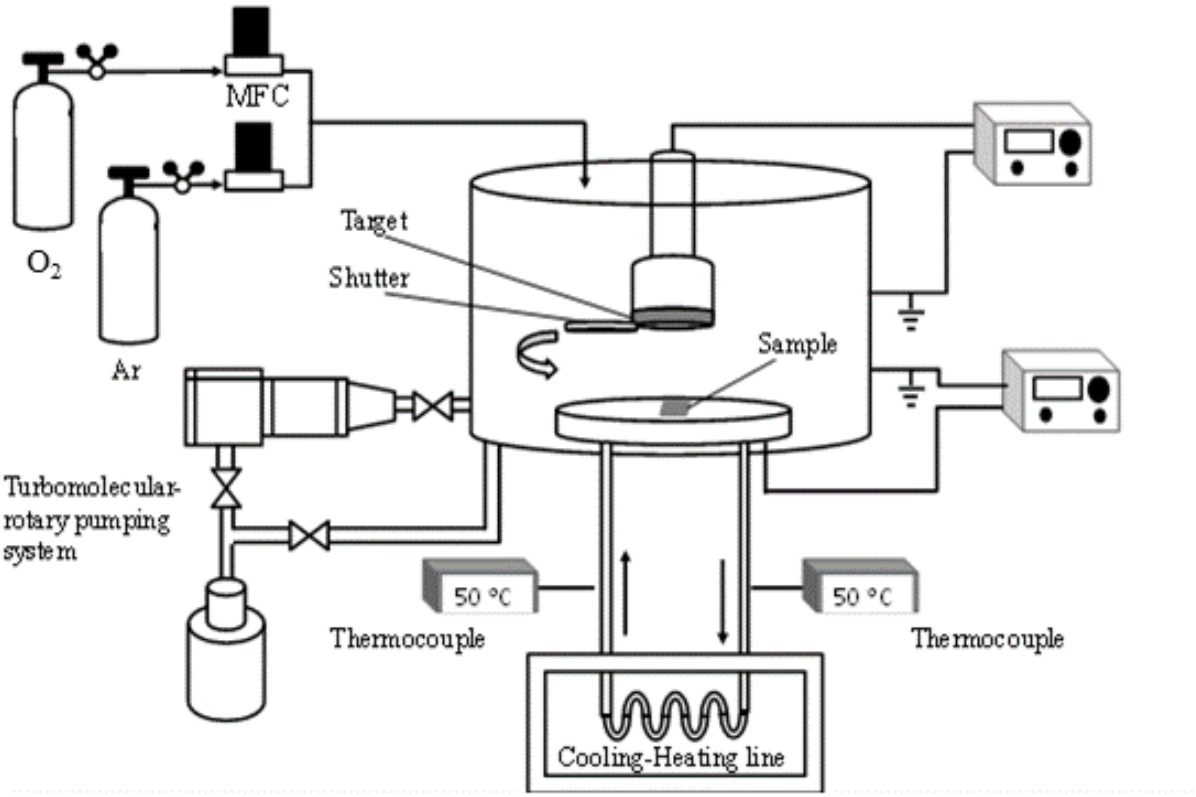

Fig 1. Scheme of the low pressure plasma reactor employed for the sputtering processes.

The magnetron source was utilized to deposit TiO_2 coatings, feeding the discharges with different argon (purity 99.999 %; *Airliquid*) and oxygen (purity 99.998 %; *Airliquid*) mixtures at 100 W of input power. Ti (purity 99.999 %; *Aja Interna-tional, Inc.*) was utilized as metal target. The gas flow rate is controlled in range 1÷200 sccm by means of mass flow controllers (*MKS Instruments, Inc.*) and the feed gases were admitted in the reactor through a ring encompassing the upper electrode.

Before the TiO_2 films deposition, a sputter cleaning process with Ar (8 sccm) at 1.33 Pa for 15 min was performed, by igniting a glow discharge at 100 W between the upper magnetron electrode and the grounded shutter plate, in order to clean the metal target. At the end of this cleaning process, the reactor was fed with the selected gas mixture, the shutter was open and the substrates were coated with the TiO_2 coatings powering the discharge at 100 W. The optimized deposition conditions are resumed in Table 1.

It is important to stress that the input power value was set at 100 W because, under this value a too slow deposition rate (estimated by thickness measurements realized employing a *Tenchor* α-step profilometer) was registered, while over 100 W a deterioration of the SB fabric was observed.

Table 1 Low pressure plasma sputtering processes experimental conditions.

Fabric type	Gas feed mixture	Pressure	Input power	Deposition time	Film thickness	Deposition rate (Rd)
A	Ar 4 sccm; O_2 4 sccm	300 Pa	100 W	180 min	93±10nm	0.52±0.05 nm/min.
B	Ar 6 sccm; O_2 2 sccm	300 Pa	100 W	180 min	81±8nm	0.45±0.04 nm/min.
C	Ar 7 sccm; O_2 1 sccm	300 Pa	100 W	180 min	65±8nm	0.36±0.04 nm/min.

2.3. Chemical characterization of the SB fabric

Before and after deposition processes, SB cellulosic fabrics were chemically and morphologically characterized by XPS measurements.

XPS analyses were performed utilizing a Scanning XPS Microprobe (PHI 5000 Versa Probe II, *Physical Electronics*) equipped with a monochromatic Al Kα X-ray source (1486.6 eV), operated at 15 kV and 24.8 W, with a spot of 100 µm. Survey (0–1300 eV) and high resolution spectra (C1s, O1s and Ti2p) were recorded in FAT (fixed analyser transmission) mode at a pass energy of 117.40 and 29.35 eV, respectively. The analyser energy resolution, evaluated on the FWHM (Full Width at half maximum) Ag $3d_{5/2}$ photoemission line, was 0.7 eV for a pass energy of 29.35 eV. Surface charging was compensated using a dual beam charge neutralization, with a flux of low energy electrons (~1 eV) combined with very low energy positive Ar^+ ions (10 eV). The hydrocarbon component of C1s spectrum was used as internal standard for charging correction and it was fixed at 285.0 eV.[32] All spectra were collected at an angle of 45° with respect to the sample surface. Atomic concentrations were determined from the high resolution spectra after subtracting a Shirley-type background, using the Scofield sensitivity factors set in the MultiPak software. For each sample, quantitative data were averaged on 9 measurements performed on three different samples.

Best-fitting of the high resolution spectra was carried out with MultiPak (*Physical Electronics*) data processing software. High resolution spectra were fitted with mixed Gaussian-Lorentzian peaks after a Shirley background subtraction.

2.4. Study of the surface wettability

The hydrophilic behaviour of the SB fabrics, before and after plasma deposition process, was evaluated by static WCA measurements, performed with a manual goniometer (*Ramé.Hart, Inc.*),

utilizing 2 µL bi-distilled water drops. The reported WCA values were averaged over 5 measurements on each fabric sample.

2.5. Photocatalytic experiments for water purification

The strain of *E. coli* ATCC 23716 (American Type Culture Collection, Rockville, MD, USA) was used. The lyophilized *E. coli* was prepared by culturing bacteria in the Brilliance *E. coli*/coliform Selective Agar (Oxoid CM1046) medium for 18-24 h at 37 °C.

Growth medium was prepared by suspending 28.1 g of Brilliance *E. coli*/coliform Selective Agar (Oxoid) in 1 L of distilled water. The medium was gently brought to a boil, to dissolve completely and autoclaved for 15 min at 121 °C. Subsequently, the medium was poured into sterile Petri dishes. Photocatalytic inactivation experiments of *E. coli* were conducted in glass beakers of 1.0 dm^3, used as batch photoreactor at lab-scale, mixing by means of a plate orbital shaker, was applied during disinfection process with UV-LED lamp placed on the top of batch reactor. For LED driven photocatalysis, an indium gallium nitride (InGaN) UVA emitter ($\lambda = 365$ nm; LZ4-00U600, LED Engin, USA) was employed and mounted onto a heat sink to prevent radiant flux decrease due to temperature rise. The LED assembly was placed directly above the reactor and a quartz protective plate was placed between them. TiO_2 fabric was immersed in 50 mL of *E. coli* solution, at the bottom of the beaker. During the experiments, samples were taken at time intervals to determine the concentration of *E. coli* in the water. The detection and quantification of bacteria, in the processing water, was performed following a standard serial dilution procedure in sterile 0.8 % (w/v %) NaCl aqueous solution and 200 µL of each dilution (including neat sample) were pipetted and spread onto Brilliance *E. coli*/Coliform Agar plates (agar plates were pre-warmed to room temperature (20 ± 5 °C) to prevent any temperature shock to the bacterial cells). Bacterial suspensions were then spread over the surface of the plate using a sterile, disposable, plastic L-shaped spreader. Agar plates were incubated at 37 °C for 18–24 h before colonies were counted. All experiments were replicated at least three times. *E. coli* colonies appeared with purple colour.

Water disinfection experiments were carried out at different initial bacterial concentrations ($10^3 – 10^8$ CFU/mL) and in different water matrices: distilled (DW), bottled (BW), 0.8% NaCl salt water (SW) and polluted water with humic acid (HA) ranging from 1 to 5 mg/L.

2.6. Photoreactivation experiments

Bacteria have the ability to repair their damaged DNA, even after their UV inactivation, through mechanisms that can occur either in the absence (dark condition) or in the presence (photo-reactivation) of light.[33]

Therefore, reactivation experiments of *E. coli* in treated waters were carried out in the dark and under natural light. In order to evaluate the photoreactivation capacity, 50 mL of the treated water was transferred, after each experimental run, into a sterile conical flask and kept in continuous agitation for 3 and 24 h, under natural light conditions and in dark conditions. Samples were analysed in terms of *E. coli* viability, with the same procedures adopted for inactivation experiments.[34]

3. Results and discussion

3.1. Chemical and morphological characterization of the TiO_2 plasma coated SB fabrics

XPS survey spectra of pristine and plasma-treated SB fabric are compared in Fig. 2. The surface of untreated SB fibers is composed by, approximately, 26 at. % of oxygen, 66 at. % of carbon, 7 at. % of silicon and 1 at. % of calcium. The spectrum of plasma-treated SB fabric is characterized by the presence of titanium beside oxygen, carbon and calcium. Depending on the conditions used, the titanium concentration is in the range 16.0-18.5 %. The presence of calcium at the surface of the SB fabric after the plasma treatment, most likely has to be ascribed to an incomplete surface coverage of the fabric by the deposited TiO_x film. In order to determine the exact film stoichiometry, i.e. the O/Ti ratio, a specific curve-fit procedure has been applied to the O1s spectra, to take into account that not all the oxygen is bound to titanium.

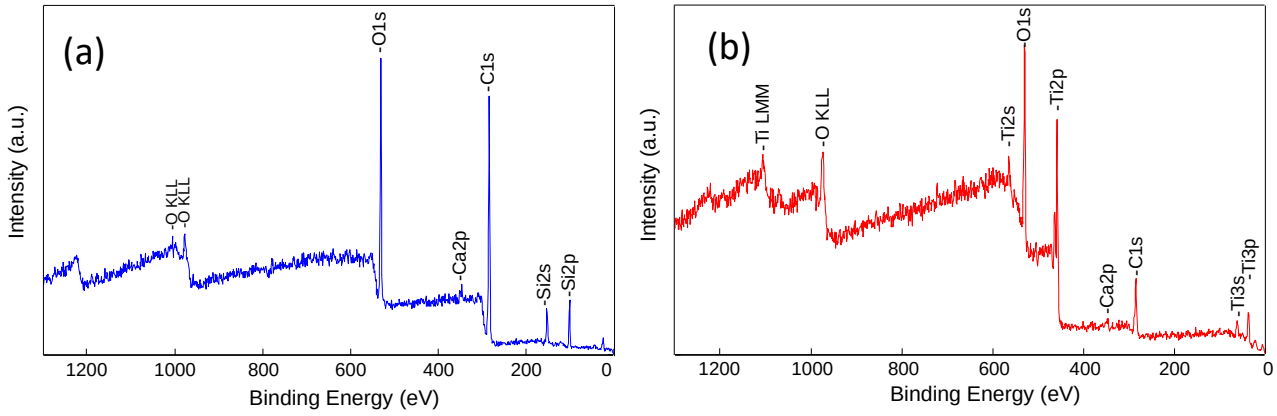

Fig 2 (a) XPS survey spectra of pristine SB fabric and (b) plasma-treated SB fabric (sample A in table 1).

Fig. 3a shows a representative curve-fitting applied to sample A (table 1). The spectrum consists of three peaks. The one set at 529.9 ± 0.1 eV is assigned to titanium oxide (TiO_x), the second peak at 531.2 ± 0.1 eV is due to titanium hydroxides, defective oxides and organic oxygen, and the third one, at 532.3± 0.1 eV, is always due to oxygen bonded in organic functional groups.[35,36] The film

stoichiometry is then calculated as the ratio between the at. % of the peak at 529.9 eV and the at. % of Ti. For all samples analysed the ratio O/Ti was found to be nearly 2. This is further confirmed by the high resolution spectra of Ti2p, shown in Fig. 3b. For all the samples the $Ti2p_{3/2}$ is set at 458.6 ± 0.1 eV, and the $Ti2p_{1/2}$ - $Ti2p_{3/2}$ splitting is 5.7 ± 0.1 eV, both values typical of TiO_2.[36] Furthermore, the spectra of Fig. 3b have identical shape and broadening confirming the same chemical environment for all the analysed samples.

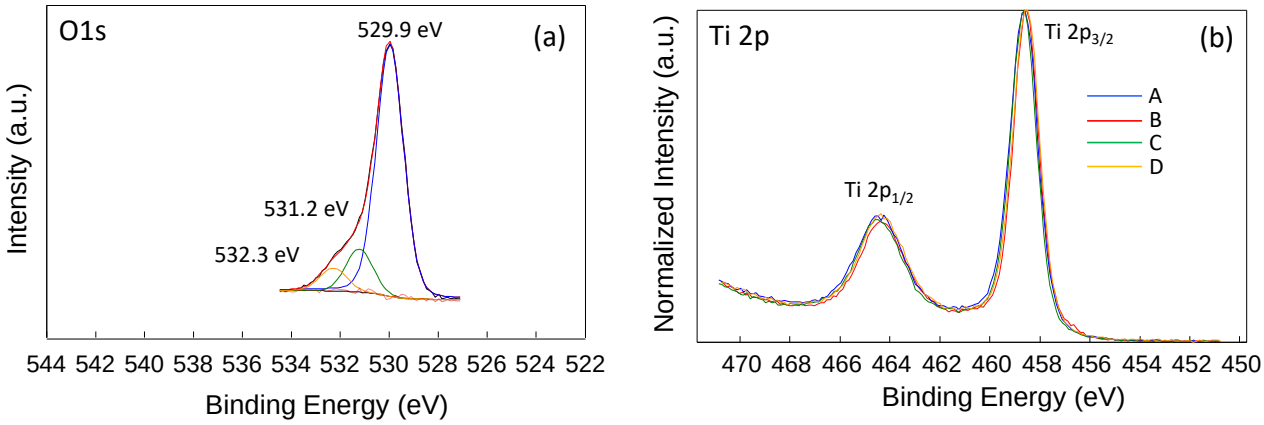

Fig. 3 (a) XPS high resolution O1s spectrum for sample A and (b) Ti2p spectra for samples A-D.

In conclusion, XPS analyses showed that in all cases the plasma treatment led to the deposition of a thin TiO_2 film, even if, the coverage of the fabric surface was not complete and, presumably, directly proportional to the oxygen content in the plasma feed gas. Observing the data reported in table 1, in fact, it is evident that the sample A was covered with the highest thickness TiO_2 layer. Sample C, on the contrary, showed the thinnest coating.

WCA measurements, performed before and after plasma TiO_2 deposition process, showed an evident increasing of the hydrophilic surface character of the SB fabric, following the plasma treatment: the WCA value, in fact, passed from 75°±3° (raw fabric) to ~ 0° (plasma TiO_2 coated sample), probably due to the grafting of oxygenated functionalities promoted by the plasma oxygen-feed glow discharges, as showed by XPS experimental results, independently by the deposition experimental conditions.

Table 2 WCA values measured on untreated and plasma treated SB fabric.

SB fabric	***WCA (°)***
Untreated	75±2

Plasma Treated	3±2

3.2. Testing the different fabric treatment for Bacterial inactivation

Bacterial degradation tests were initially carried out by maintaining the same experimental conditions, in order to identify the best grafted fabric among those prepared under different plasma conditions. The initial concentration of *E. coli* in distilled water was 10^4 CFU/mL. To evaluate the photolytic capacity of the UV-LEDs system, tests were also carried out in the absence of any antimicrobial fabric. Fig. 4 shows the kinetics of photocatalytic bacterial inactivation as a function of the UV exposure time, obtained in the presence of several TiO_2-deposited cellulose fabrics and compares them with that obtained by UV exposure only. It can be seen that UV exposure alone induces bacterial inactivation leading to a 49% reduction of the bacterial population after 90 min. However, it is a very slow process compared to the inactivation kinetics observed when the fabric photocatalyst is placed into the reactor. In this case, the 50% bacterial inactivation is achieved after about 10 min of UV irradiation, while 100% inactivation occurs after about 30-60 min, depending on the used fabric.

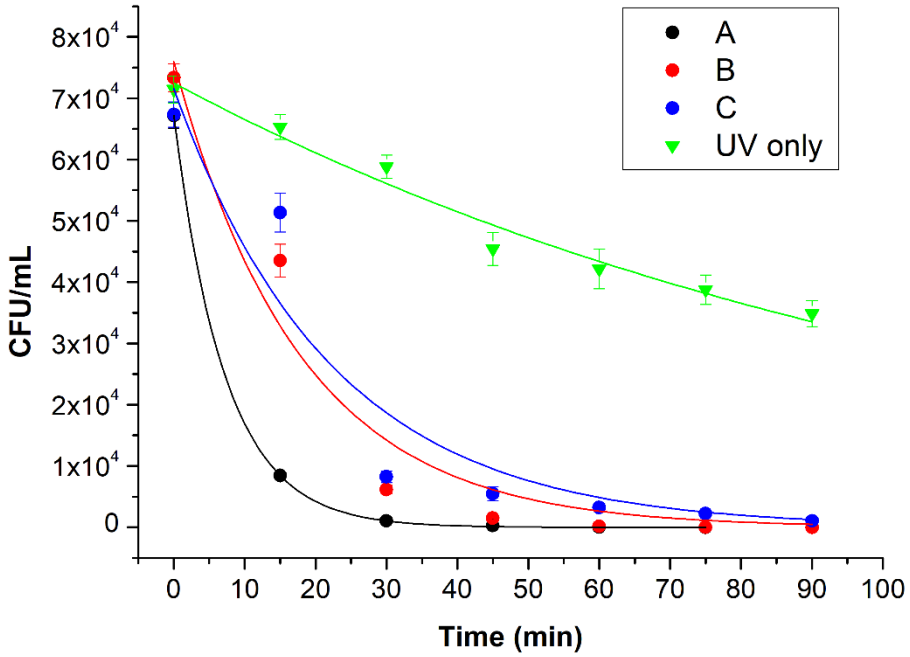

Fig. 4 Kinetics of photocatalytic inactivation by different TiO_2-cellulose fabrics at a UV-LED wavelength exposure of 365 nm. Lines are the best fit of the data by a first order law.

Indeed, Fig. 4 shows that the photocatalytic inactivation kinetics significantly depends on the fabric processing (see Table 1) and increases in the following order: fabric A > fabric B ≥ fabric C. As described in the previous section, the above trend corresponds to the increase of the thickness, and

probably to a more homogeneous coating, of TiO_2 film deposited on the fabric surface, passing from deposition condition A to the deposition condition C. The kinetics of *E. coli* inactivation follows a first order reaction with respect to the concentration of viable cells in the reactor as expressed by equation (1):

$$\frac{N_t}{N_0} = e^{-kt} \qquad (1)$$

where, N_t is the residual microbial load at a given time (CFU/mL), N_0 is the initial microbial load (CFU/mL), k is the inactivation rate constant (m^2/kJ or min), t is the UV treatment time.

Fig. 4 reports the fitting lines for each set of kinetic data. The fitting results, reported in Table 3, show that the rate constant obtained with fabric A is from 2.5 up to 3 times higher than the one observed with fabrics B and C, respectively, and more than one order of magnitude larger than that of the UV exposure treatment alone.

Table 3 First order kinetic rate constant of the photocatalytic bactericidal activity of TiO_2- coated fabrics in various water matrices compared to photolytic treatment

Inactivation experiment	**Water matrix**	**N_0 (× 10^4 CFU/mL)**	**k (s^{-1})**	**R^2**
UV only	DW	7.2	0.0090 (0.0006)	0.970
Fabric C		7.2	0.045 (0.009)	0.903
Fabric B		7.6	0.055 (0.009)	0.949
Fabric A		6.7	0.138 (0.001)	0.99996
		4670	0.096 (0.007)	0.9939
		0.66	0.115 (0.006)	0.99815
	BW	7.1	0.111 (0.001)	0.99989
	SW	7.4	0.088 (0.002)	0.99943
	1 mg/L HA	6.6	0.067 (0.002)	0.99827
	2 mg/L HA	6.0	0.053 (0.003)	0.9944
	5 mg/L HA	7.1	0.041 (0.003)	0.98491

Fig. 5 reports the inactivation kinetics obtained by using Fabric A on E. coli suspended in distilled water (DW) as a function of the initial bacterial concentration (10^3 - 10^8 CFU/mL). It clearly shows

that the kinetic constant is independent on N_0 being the other experimental conditions the same (i.e. type of fabric, water matrix, temperature, UV exposure). From Table 3, an average *k* value of 0.12 ± 0.02 can be calculated, in this case. Interestingly, the inactivation kinetics in bottled water (BW) is the same as that in DW due to the low concentration of dissolved substances in this natural mineral water sample.

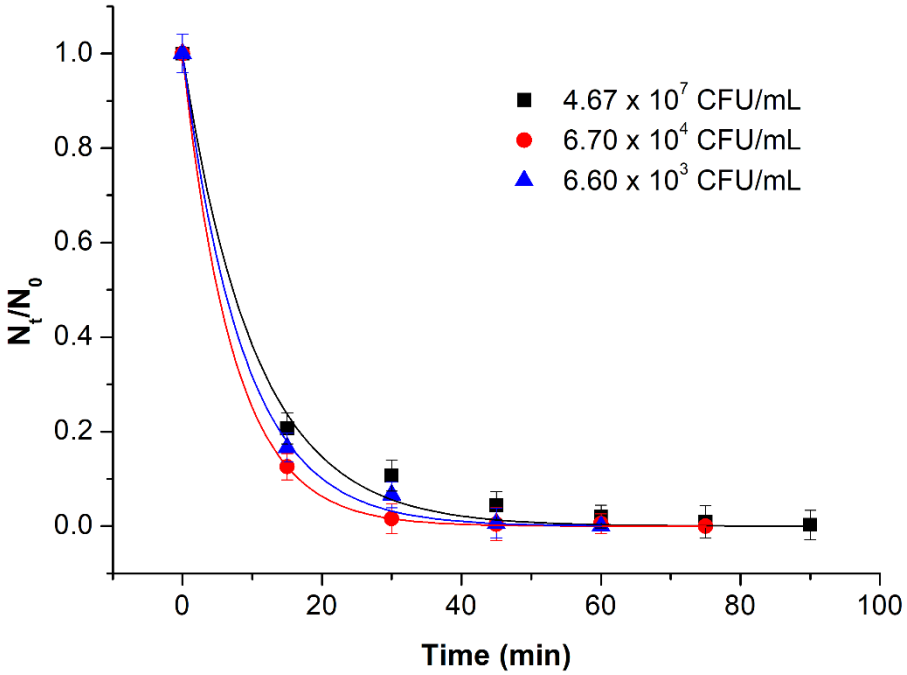

Fig. 5 Effect of initial bacterial concentration.

3.3. Effect of water matrix

The photocatalytic bacterial inactivation effect has been further evaluated in different water matrices other than in distilled water (DW): bottled water (BW), 0.8% NaCl salt water (SW) and water spiked with various concentrations of humic acid (HA), ranging from 1 to 5 mg/L, in order to resemble more realistic surface water and wastewater treatment conditions.

All water matrices were spiked with an initial bacterial concentration of 6-8 × 10^4 CFU/mL and treated by fabric A. The inactivation kinetics measured in the different water matrices are displayed in Fig. 6.

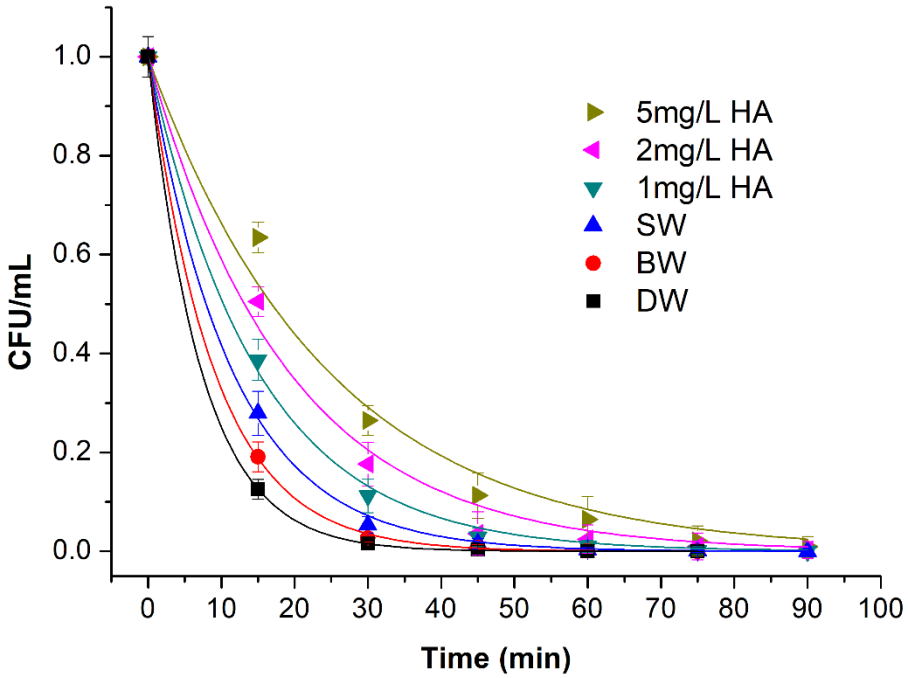

Fig. 6 Kinetics of photocatalytic bacterial degradation in different water matrices.

A first order inactivation kinetics was also observed in all the water matrices under investigation, with the rate constants reported in Table 3. As already discussed above, the kinetics of bacterial inactivation in BW is analogous with respect to that observed in DW. However, upon addition of 0.8% of NaCl in DW, bacterial inactivation becomes significantly slower. This may be due to the fact that bacteria are suspended in an aqueous medium with physiologic osmolarity where any osmotic stress condition does not add up to the stress induced by UV exposure and the photocatalytic process. Interestingly, the inactivation kinetics becomes progressively slower when *E. coli* are incubated in an aqueous medium contaminated with increasing concentration of humic acids (Fig. 6). This effect can be explained by considering at least three mechanisms:[37-39] 1) HA can form a UV absorbing layer by coating the bacteria surface, which would act as a shield against UV exposure. This mechanism can occur at ratios between the mass of HA and the cfu smaller than 1 ng HA/cfu[37], as in our experimental conditions (Fig. 6); 2) organic compounds, like HA, can compete with bacteria for reactive oxygen species (ROS), thus reducing the photocatalytic activity against bacteria inactivation[38]. 3) A decrease of the UV inactivation efficiency in the presence of HA could be due to a microorganism growth promoting effect of HA.[39] We have in fact, observed that HA promotes the growth of E. Coli in samples previously inactivated (Table 4). Nevertheless, the kinetic of growth (10^2/day see Table 5) is much slower than that of the photocatalytic inactivation ($5x10^7$/h; see Table 3). Therefore, we believe that, among the above three mechanisms possibly contributing to the HA induced slowdown effect on the inactivation kinetics, the latter could be neglected with respect to the first two ones.

3.4. Inactivation efficiency

Log inactivation is another way of indicating the level of disinfection occurred following UV treatment. Log inactivation was calculated by Eq. (2):

$$\textbf{Log inactivation} = \log N_0/N_t \qquad (2)$$

where, N_0 and N_t having the usual meaning.

The inactivation efficiency of different UV inactivation methods, can be compared by taking into account the Dose response (mJ/cm^2 per log inactivation) which is the UV irradiation dose (mJ/cm^2) normalized with respect to the log inactivation. The UV dose and the Dose response are defined by the equation (3) and (4), respectively.

$$\textbf{UV dose} = I \times t \qquad (3)$$

$$\textbf{Dose response} = \textbf{UV Dose} / \textbf{Log inactivation} \qquad (4)$$

where, I is the UV power density (mW/cm^2), t is the irradiation time (s).

Table 4 reports the dose response values obtained in this study in the two extreme cases discussed above, i.e., at the highest log inactivation in DW and at the lowest log inactivation in 5 mg/L HA solution. These values are compared to the dose response obtained in this work under UV exposure without fabric and with other dose response values reported in the literature. It can be seen that the bacterial inactivation efficiency in the presence of the TiO_2-coated fabric is from about 4 up to 17 times higher than that of UV irradiation only, which clearly indicates the occurrence of the photocatalytic mechanism due to the presence of the fabric. Overall, Table 4 shows that the photocatalytic inactivation system proposed here is very efficient because the dose response is one of the lowest if compared to that obtained with other UV methods which do not utilize the photocatalytic process induced by the TiO_2 layer. Table 4 reports also the data related to the inactivation of E. coli with UV at 365 nm in a water/TiO_2 medium[9] with a dose response as low as 229 mJ/cm^2, which is about 30 times smaller than that obtained in this work. However, a direct comparison between these two methods can be hardly done without considering the experimental exposure set-up used, in particular the ratio between the TiO_2 photocatalytic surface layer and the volume of bacterial suspension which determines the film water thickness in contact with the photocatalytic layer. Xiong

and Hu (2013) used a TiO_2 –coated (15 μm thickness) crystallizing dish with a diameter of 10 cm and a suspension volume of 30 mL. Under these conditions, the film suspension thickness was about 0.4 cm while, in our experiment, it was about 10 times larger. It is clear that in the conditions used by Xiong and Hu (2013), the photocatalytic inactivation efficiency was maximized with respect to the exposure conditions but, this was achieved at a very high TiO_2 surface layer/volume suspension ratio, which is hardly applicable in practice.

Table 4 Inactivation efficiency of the method proposed in this work compared to other ones

UV Technology	Wavelength (nm)	UV dose (mJ/cm^2)	Log inactivation	Dose response (mJ/cm^2 per log inactivation)	Reference
UV-LED lamp only	365	36,000	0.3	120,000	This study
TiO_2 coated fabric (DW)	365	36,000	4.9	7,347	This study
TiO_2 coated fabric (5 mg/L HA)	365	57,200	2.04	28,039	This study
Sterilization device	365	54,000	3.9	13,846	[40]
UV-A system	365	315,000	5.7	55,263	[8]
UV-LED system	385	576,000	3.8	151,579	[41]
Crystallizing dish coated with TiO_2	365	688	3	229	[9]

3.5. Photoreactivation experiments

In order to evaluate the efficacy of UV treatment, experiments of bacterial photoreactivation were carried out on previously decontaminated aqueous matrices. The results, reported in Table 5, show that the reactivation of E. Coli is absent after 3 and 24 hours of exposure to natural light and dark condition in all matrices, except for those containing humic acid at 2 and 5 mg/L. In these cases we

observed a bacteria regrowth of less than 150 CFU/mL, both in presence and in the absence of light, even after 24 h.

Table 5 E. coli photoreactivation experiments, under natural light and dark conditions, in UV inactivated waters

Fabric A Experiments	**E. Coli initial concentration (CFU/mL)**	**UV treatment time for inactivation of E. Coli (CFU/mL)**	**E. Coli survival after 3h of photoreactivation (CFU/mL)**		**E. Coli survival after 24h of photoreactivation (CFU/mL)**	
			LIGHT	*DARK*	*LIGHT*	*DARK*
Distilled water	10^3	60 min	nd [a]	nd	nd	nd
	10^4	75 min	nd	nd	nd	nd
	10^8	120 min	nd	nd	nd	nd
Bottled water	10^4	75 min	nd	nd	nd	nd
Salt water	10^4	90 min	nd	nd	nd	nd
1 mg/L HA	10^4	90 min	nd	nd	nd	nd
2 mg/L HA	10^4	120 min	nd	nd	<100	<100
5 mg/L HA	10^4	120 min	<100	<100	100-150	100-150

[a] not detected

3.6. Reuse of plasma coated SB fabric

The recycling and/or re-use of photocatalytic material reduces the operating costs and the environmental impact. Therefore, reusability studies are important for assessing the potential of large-scale applications of the developed technology.

A simple regeneration process was carried out by washing the surface of the plasma TiO_2-coated SB fabrics with ultrapure water and drying it at a temperature of 90°C for 60 min before any subsequent tests. The photocatalytic effect of the regenerated fabric has been evaluated under the same experimental conditions used in the DW experiments described above. The experimental results are shown in Fig. 7, where it can be observed that the regenerated fabric shows satisfactory reusability, since its bacterial inactivation capacity is very close to that of the original fabric, also after the second regeneration process and the following third use.

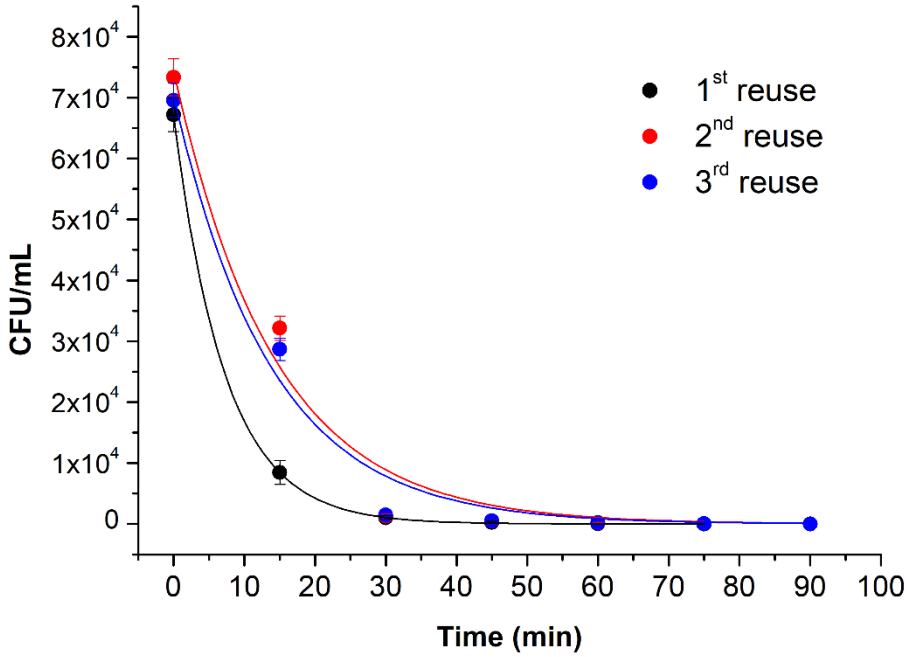

Fig. 7 Bacterial degradation experiments for reuse purposes.

The only difference is found in the first few minutes of treatment, in which the bacterial inactivation performed by the reused fabrics is slower (the *k* goes from 0.138 for the first use, to 0.07 s^{-1} for the second and third (Table 6)). Nevertheless, complete inactivation of the bacteria still occurs within 90 min of treatment.

Table 6 First order kinetic rate constant of the photocatalytic bactericidal activity of TiO_2-coated fabrics for reusability experiments.

Experiment	**N_0 (CFU/mL)**	**k (s^{-1})**	**R^2**
1st use	67170 (71)	0.138 (5,467E-4)	0.999
2nd reuse	74513 (4619)	0.07 (0,009)	0.973
3rd reuse	70469 (3806)	0.07 (0,009)	0.979

The slight loss of the fabric catalytic activity is probably due to the regeneration method. The reduction of the bacterial inactivating capacity is ascribable to the not fully effective regeneration and washing method, as supported by XPS analyses results performed on SB plasma modified fibers after each regeneration/use cycle. Data of Table 7 (XPS surface atomic percent of recycled SB plasma

modified samples), in fact, show that the atomic percent of titanium and oxygen decrease, while that of carbon increases.

Table 7 XPS atomic percent of plasma coated SB fiber as deposited and after different regeneration/use cycle.

Sample	C at. %	O at.%	Ti at.%
As deposited	33.3	50.5	16.2
After 1 use	48.2	44.4	7.4
After 2 use	52.1	41.3	6.6
After 3 use	59.7	36.9	3.4

This could point out to a potential leaching of the catalyst with use, but, if the elemental high resolution spectra are analyzed (Fig. 8), it is evident that Ti chemical environment do not change with use, since the overall shape, main peak position ($Ti2p_{3/2}$) and $Ti2p_{1/2}$ - $Ti2p_{3/2}$ splitting stay the same. Thus, it can confirm that the catalyst is stable over time.

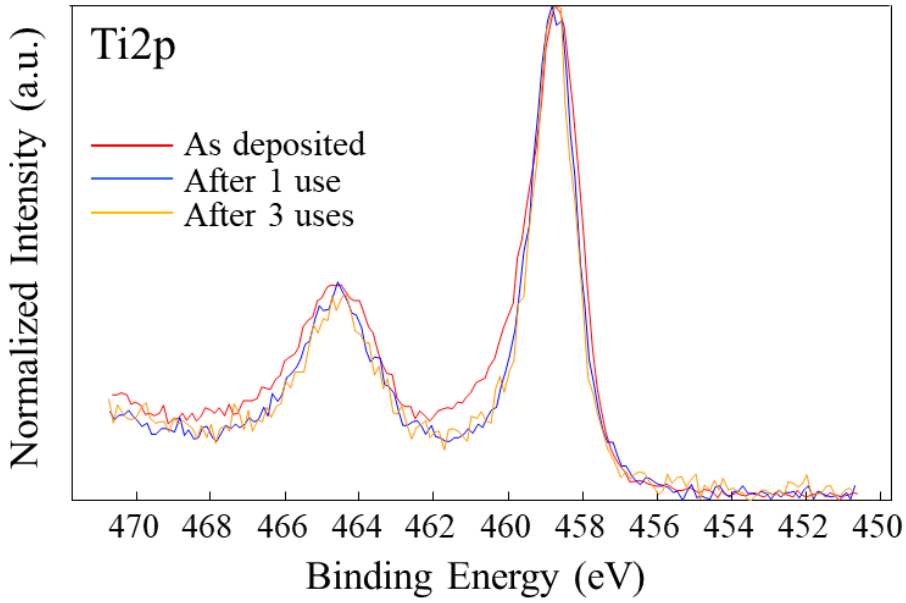

Fig. 8 Ti2p XPS high resolution spectra acquired after SB plasma modified fiber use.

This hypothesis was supported also by C1s spectrum analysis, which reveals some changes in the carbon chemical environment (Fig. 9): the C1s spectrum of the as deposited sample A resembles that

of untreated SB fabric. After the use, on the contrary, the spectra show that the relative contribution between 286 and 287 eV increase, likely due to the uptake from the solution environment used for testing. Therefore, it can be asserted that the decrease in titanium atomic percent is not due to a dissolution of the catalyst, but rather to a carbon uptake from the environment.

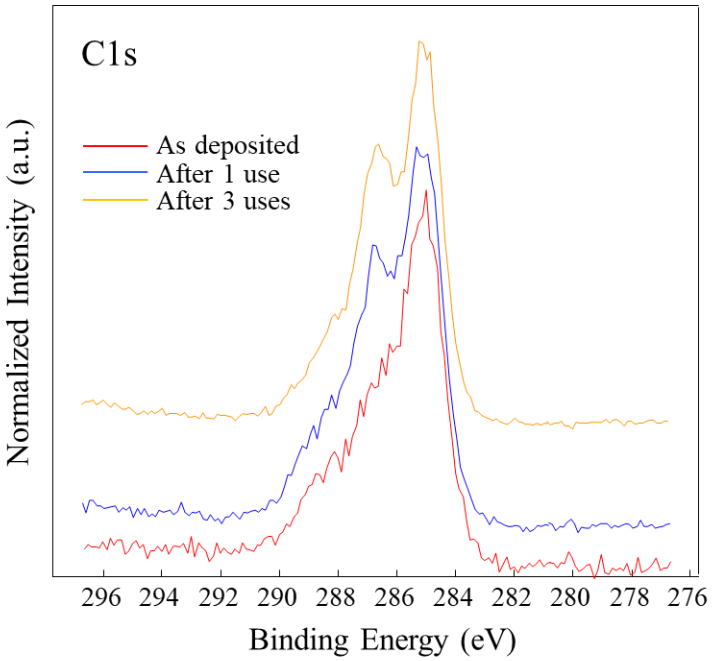

Fig. 9 C1s spectra of as deposited and after recycle sample A.

Further catalyst regeneration tests could be carried out, varying the method, the solvent and the duration of the washing in order to improve the recycle protocol, totally preserving the catalytic activity of the as deposited plasma TiO_2 covered SB fabric.

4. Conclusions

This work reports the first application of TiO_2 plasma coated biobased fabric, obtained from Spanish broom cellulose fibers, to disinfect water from *E. coli* bacteria.

The functionalized cellulose fabric exhibited very good disinfection capacity for concentration of *E. coli* from 10^3 to 10^8 CFU/mL in water. Bacteria have been inactivated after 60-75 min of treatment time under UV-LED irradiation. First order inactivation kinetics were observed in all of the water matrices considered. The rate constant obtained with fabric A is more than one order of magnitude larger than that obtained after photolytic treatment. It has been also observed that the photocatalysts are stable after several reuse cycles and can be easily regenerated by a simple and fast washing process which allows to maintain a disinfection capacity very close to the initial one.

In conclusion, the results obtained from this study indicate the potential disinfectant capacity of this material. The technology could be applicable on a large scale, due to the high availability of cellulose from Spanish broom plants and the low-cost scalable process of functionalization.

On the other hand, according to previous reports, it is expected that this technology could be also applied to viral strain inactivation.[42,43]

Moreover, unlike conventional methods of bacterial disinfection, the proposed application has the advantage of the absence of by-products during its use and the ability to perform catalytic activity through the application of lower-energy UV wavelengths.

Conflicts of interest

There are no conflicts to declare

Acknowledgements

This research was also financially supported by Regione Puglia under grant no. 51 “Laboratorio pubblico di ricerca industrial dei plasmi, LIPP”, within the Framework Programme Agreement APQ “Ricerca Scientifica”, II atto integrativo - Reti di Laboratori Pubblici di Ricerca and by PON “R&C” 2007-2013 - Avviso n.254/Ric del 18 maggio 2011 PONa3_00369 “Laboratorio per lo Sviluppo Integrato delle Scienze e delle TEcnologie dei Materiali Avanzati e per dispositivi innovativi (SISTEMA).

References

1 WHO, *Progress on Drinking Water and Sanitation*, World Health Organization and Unicef, Switzerland, 2014. ISBN 978 92 4 150724 0.

2 C. Regmi, B. Joshi, S. K. Ray, G. Gyawali and R. P. Pandey, Understanding Mechanism of Photocatalytic Microbial Decontamination of Environmental Wastewater, Front. Chem., 2018, 6, 33.

3 M. N. Chong, B. Jin, H. Zhu and C. Saint, Bacterial inactivation kinetics, regrowth and synergistic competition in a photocatalytic disinfection system using anatase titanate nanofiber catalyst. J. Photochem. and Photobio. A: Chem., 2010, 214, 1–9.

4 A. R. Rahmani, A. J. Jafari and A. H. Mahvi, Investigation of water disinfection by electrocd, Pakistan of Biol. Sci., 2005, 8, 910- 913.

5 R. T. Bisneto and E. Bidoia, Effects of the electrolytic treatment on bacillus subtilis, Brazilian J. Microbiol., 2003, 34, 48-50.

6 K.Y. Nelson, D. W. McMartin, C. K. Yost, K. J. Runtz and T. Ono, Point-of-use water disinfection using UV light-emitting diodes to reduce bacterial contamination, Environ. Sci. Pollut. Res. Int., 2013, 20, 5441-5448.

7 P.O. Nyangaresi, Y.Qin, G. Chen, B. Zhang, Y. Lu and L. Shen, Effects of single and combined UV-LEDs on inactivation and subsequent reactivation of E. coli in water disinfection, Water Res., 2018, 147, 331-341.

8 A. Hamamoto, M. Mori, A. Takahashi, M. Nakano, N. Wakikawa, M. Akutagawa, T. Ikehara, Y. Nakaya and Y. Kinouchi, New water disinfection system using UVA light-emitting diodes, J. Appl. Microbiol., 2007, 103, 2291-2298.

9 P. Xiong and J. Y. Hu, Inactivation/reactivation of antibiotic-resistant bacteria by a novel UVA/LED/TiO2 system, Water Res., 2013, 47, 4547-4555.

10 S. Anandan, Y. Ikuma and K. Niwa, An Overview of Semi-Conductor Photocatalysis: Modification of TiO2 Nanomaterials, Solid State Phenom., 2010, 162, 239-260.

11 D. S. Bhatkhande, V. G. Pangarkar and A. C. M. Beenackers. Photocatalytic degradation for environmental applications – a review, *J. Chem. Technol. Biotechnol.*, 2001, **77**, 102-116.

12 T. V. Nguyen and J. C. S. Wu, Photoreduction of CO2 in an optical-fiber photoreactor: Effects of metals addition and catalyst carrier, *Appl. Catalysis A: General.*, 2008, **335**, 112–120.

13 M. Janus, A. Markowska-Szczupak, E. Kusiak-Nejman and A. W. Morawski, Disinfection of E. coli by carbon modified TiO2 photocatalysts, *Environ. Prot. Eng.*, 2012, **38**, 89–97.

14 P. Wu, R. Xie, K. Imlay and J. K. Shang, Visible-Light-Induced bactericidal activity of titanium Dioxide codoped with Nitrogen and Silver, *Environ. Sci. Technol.*, 2010, **44**, 6992-6997.

15 W. C. Oh, A. R. Jung and W. B. Ko, Characterization and relative photonic efficiencies of ZnO-coated multi-walled carbon nanotubes, *Mater. sci. eng.*, 2009, **29**, 1338-1347.

16 V. Krishna, S. Pumprueg, S. H. Lee, J. Zhao, W. Sigmund, B. Koopman and B. M. Moudgil, *Trans. IchemE, Proc. safety environ. prot.*, 2005, **83**, 393.

17 O. Akhavan, M. Abdolahad, Y. Abdi and S. Mohajerzadeh, Synthesis of titania/carbon nanotube heterojunction arrays for photoinactivation of E. coli in visible light irradiation, *Carbon*, 2009, **47**, 3280- 3287.

18 G. Dagan and M. Tomkiewicz, TiO2 aerogels for photocatalytic decontamination of aquatic environments, *J. Phys. Chem.*, 1993, **97**, 12651-12655.

19 D. Sethi, N. Jada, A. Tiwari, S. Ramasamy, T. Dash and S. Pandey, Photocatalytic destruction of Escherichia coli in water by V2O5/TiO2, *J. Photochem. Photobiol. B*, 2015, **144**, 68–74.

20 B. Gabriele, T. Cerchiara, G. Salerno, G. Chidichimo, M. V. Vetere, C. Alampi, M. C. Gallucci, C. Conidi and A. Cassano, A new physicalechemical process for the efficient production of

cellulose fibers from Spanish broom (Spartium junceum L.), *Bioresour. Technol.*, 2010, **101**, 724-729.

21 F. Arias, A. Beneduci, F. Chidichimo, E. Furia and S. Straface, Study of the adsorption of mercury (II) on lignocellulosic materials under static and dynamic conditions, *Chemosphere*, 2017, **180**, 11-23.

22 A. Tursi, A. Beneduci, F. Chidichimo, N. De Vietro and G. Chidichimo, Remediation of hydrocarbons polluted water by hydrophobic functionalized cellulose, *Chemosphere*, 2018, **201**, 530-539.

23 A. Tursi, E. Chatzisymeon, F. Chidichimo, A. Beneduci and G. Chidichimo, Removal of Endocrine Disrupting Chemicals from Water: Adsorption of Bisphenol-A by Biobased Hydrophobic Functionalized Cellulose, *Int J. Environ. Res. Public Health*, 2018, **15**, 2419.

24 N. De Vietro, L. Belforte, V. G. Lambertini, F. Fracassi, Low pressure plasma modified polycarbonate: A transparent, low reflective and scratch resistant material for automotive applications, *Appl. Surf. Sci.*, 2014, **307**, 698-703.

25 L. D'Accolti, N. De Vietro, F. Fanelli, C. Fusco, A. Nacci and F. Fracassi, Heterogenization of Ketone Catalyst for Epoxidation by Low Pressure Plasma Fluorination of Silica Gel Supports, *Molecules*, 2017, **22**, 1-14.

26 N. De Vietro, C. Annese, L. D'Accolti, F. Fanelli, C. Fusco and F. Fracassi, A new synthetic approach to oxidation organocatalysts supported on Merrifield resin using plasma-enhanced chemical vapor deposition, *Appl. Catal. A*, 2014, **470**, 132– 139.

27 N. De Vietro**,** R. d'Agostino and F. Fracassi, Introduction of basic functionalities on the surface of granular adsorbers by low pressure plasma processes, Plasma Process. Polym.**,** 2012, **9**, 911-918.

28 N. De Vietro, R. d'Agostino and F. Fracassi, Improvement of the adsorption properties of carbon black granules by means of plasma enhanced-chemical vapour deposition with acrylic acid vapours, *Carbon*, 2011, **49**, 249-255.

29 N. De Vietro, in Carbon black: production, properties and uses, ed. I. J. Sanders and T. L. Peeten, Nova Science Publishers, USA, 2011, 10, 237-262.

30 N. De Vietro, A. Conte, A.L. Incoronato, M.A. Del Nobile and F. Fracassi, Aerosol-assisted low pressure plasma deposition of antimicrobial hybrid organic-inorganic Cu-composite thin films for food packaging applications. *Innov. Food Sci. Emerg. Technol.*, 2017, **41**, 130–134.

31 F. Fanelli, A. M. Mastrangelo, N. De Vietro and F. Fracassi, Preparation of multifunctional superhydrophobic nanocomposite coatings by aerosol-assisted atmospheric cold plasma deposition, *Nanosci. Nanotechnol. Lett.*, 2015, **7**, 84-88.

32 G. Beamson and D. Briggs, High Resolution XPS of Organic Polymers: The Scienta ESCA300 Database, *J. Chem. Educ.*, 1993, **70**, A25.

33 E. Chatzisymeon, A. Droumpali, D. Mantzavinos and D. Venieri, Disinfection of water and wastewater by UV-A and UV-C irradiation: Application of real-time PCR method, *Photoch. Photobio. Sci.*, 2011, **10**, 389-95.

34 E. Chatzisymeon, Inactivation of bacteria in seafood processing water by means of UV treatment, *J. Food Eng.*, 2016, **173**, 1-7.

35 C. D. Wagner, W. M. Riggs, L. E. Davis, J. F. Moulder and G. E. Muilenberg, *Handbook of X-Ray Photoelectron Spectroscopy*, Perkin-Elmer Corporation, Minnesota, 1979.

36 M. C. Biesinger, L. W. M. Lau, A. R. Gerson, R. S. C. Smart, Resolving surface chemical states in XPS analysis of first row transition metals, oxides and hydroxides: Sc, Ti, V, Cu and Zn, *Appl. Surf. Sci.*, 2010, **257**, 887-898.

37 R. E. Cantwell, R. Hofmann, M.R. Templeton, Interactions between humic matter and bacteria when disinfecting water with UV light, *J. Appl. Microbiol.*, 2008, **105**, 25–35. https://doi.org/10.1111/j.1365-2672.2007.03714.x

38 D. M. A. Alrousan, P. S. M. Dunlop, T. A. McMurray, J. A. Byrne, Photocatalytic inactivation of E. coli in surface water using immobilised nanoparticle TiO2 films, *Water Res.*, 2009, **43**, 47–54.

39 E. Lee, H. Lee, W. Jung, S. Park, D. Yang, K. Lee, Influences of humic acids and photoreactivation on the disinfection of Escherichia coli by a high-power pulsed UV irradiation, *Korean J. Chem. Eng.*, 2009, **26**, 1301-1307.

40 M. Mori, A. Hamamoto, A. Takahashi, M. Nakano, N. Wakikawa, S. Tachibana, T. Ikehara, Y. Nakaya, M. Akutagawa, Y. Kinouchi, Development of a new water sterilization device with a 365 nm UV-LED. *Med. Biol. Eng. Comput.*, 2007, **45**, 1237-1241.

41 S. A. Malik, T. T. Swee, N. A. N. N. Malek, M. R. A. Kadir, T. Emoto, M. Akutagawa, L. K. Meng, T. Hou, T. A. I. T. Alang, T.A., Comparison of standard light-emitting diode (LED) and 385 nm ultraviolet A LED (UVA-LED) for disinfection of Escherichia coli, *Mal. J. Fund. Appl. Sci.*, 2007, **IMEDITECH**, 430-437. DOI: https://doi.org/10.11113/mjfas.v13n4-2.758

42 X. Sang, T. G. Phan, S. Sugihara, F. Yagyu, S. Okitsu, N. Maneekarn, W. E. Müller, H. Ushijima, Photocatalytic inactivation of diarrheal viruses by visible-light-catalytic titanium dioxide, *Clin. Lab.*, 2007, **53**, 413-421.

43 D. Gerrity, H. Ryu, J. Crittenden, M. Abbaszadegan, Photocatalytic inactivation of viruses using titanium dioxide nanoparticles and low-pressure UV light, *J. Environ. Sci. Health A Tox. Hazard Subst. Environ. Eng.*, 2008, **43**, 1261-1270.